Sliding Mode Control for DC Motor System with Multi-channels and External Disturbances

Longyu Xu, Yong Chen, *Senior Member*, *IEEE* and Meng Li

***Abstract*—In order to solve the deficiencies of speed tracking control for DC motor system with multiple transmission channels and external disturbances in recent remote-control systems, a second-order super twisting sliding mode control (SSTSMC) method is proposed. Firstly, the model of DC motor with multiple channels and external disturbances is considered. Then, an observer in the form of super twisting algorithm (STA) is presented to estimate the states of system. Furthermore, a SSTSMC algorithm based on the super twisting observer (STO) is designed to track the speed of the DC motor. In which, a nonlinear term is constructed so as to restrain the external disturbances and jitters while switching among the channels. Also, the proposed method is testified to be stable. Finally, both simulations and practical experiments are conducted to demonstrate the availability of the methodology.**

***Index Terms*—Speed tracking of DC motor, multiple channels, external disturbances, STO, and SSTSMC.**

I. Introduction

DC motor has been diffusely applied in satellite，aerospace, robot control and other fields due to its good speed regulation performance and dynamic characteristics [1]. With the rapid development of military, medical and industrial control fields, in recent years, the accuracy and response speed of DC motor speed control requirements are increasingly higher, which has widely aroused the scholars' keen attention. Furthermore, in modern industrial control systems, the parameters of the controlled objects are usually gathered by multiply sensors and transferred through different channels [2].

The switch of sensors and channels will inevitably introduce abrupt parameter variation so that markov jump theory can be used effectively in such systems. In [3], a hidden Markov model is proposed in order to deal with the possible asynchronous asymmetry between the system mode and the controller mode, and cause the closed-loop system to follow a hidden Markov motion. In [4], a robust controller for a networked control system of multiple communication channels is developed, in which the Markov channel switching algorithm is applied. In [5], an equivalent control method for MIMO uncertain linear Markov jump systems based on sliding mode control is designed to make sure that the system is stochastic asymptotic stable. Hence, introducing Markov jump to deal with the problem of switching among multiple channels is theoretical probable.

As for the problem of control system, various advanced control algorithms have been proposed. For example, PID control [6], h-infinity control [7-8], fuzzy control [9-10], model predictive control [11-12], event-triggered control [13-14], sliding mode control (SMC) [15-16], etc. In which, SMC has the advantages of simple algorithm, strong robustness and fast response, which can overcome the uncertainty of the system and be suitable for nonlinear systems. Some scholars have applied the SMC method to space robot control. SMC is a significant methodology for nonlinear control, as a result of which, it has been diffusely researched recently. However, the shortcomings of SMC are also obvious. When the motion trajectory of the SMC moves close to the sliding surface, it usually moves back and forth within the sliding mode bandwidth, instea1d of directly moving to the equilibrium point, which is also the main problem in practical applications.

In order to damp out the jitters, there have been many researches so far, including high-order SMC, adaptive SMC, etc. In [16], Xu proposes a SMC strategy based on terminal sliding mode surface, which designs a new second-order discrete-time SMC strategy for precision motion control of piezoelectrically driven Nano-positioning devices. This strategy is easy to realize and eliminate the use of state observer by using the feedback of output value. In [17], an integral suboptimal second-order SMC algorithm is proposed. The algorithm adjusts the controller, which different from conventional SMC, is continuous control output to the system so that it can be better applied into industrial robot operation. This algorithm has positive damping effect and is proved to be able to use in industry. In [18], in order to control the wind energy conversion system between generator and grid sides, Merabet et al. design a SMC method. The method is based on external disturbance model and is of great robustness. Experiments in which show that the proposed method is robust to the uncertain disturbances, changing parameters and system uncertainness.

The above-mentioned method is effective to control the corresponding systems. However, the chattering is still not greatly damped and the methods cannot be fast transplanted into other aspects. Hence, some scholars propose to introduce a nonlinear term into the control strategy, where STA is a popular

This work was supported by the National Natural Science Foundation of China under Grant (61903064 and 61973331), the China Postdoctoral Science Foundation funded project under Grant (2019M663479), the National Key Research and Development Plan Programs of China under Grant (2018YFB0106101), the Fundamental Research Funds for the Central Universities under Grant (ZYGX2019J058), and the Postdoctoral Fund Project of University of Electronic Science and Technology of China (UESTC) under Grant (Y03019023601016200).

The authors are with the School of Automation Engineering, University of Electronic Science and Technology of China, Chengdu, Sichuan 611731, China (email: ronnri331@gmail.com; ychencd@uestc.edu.cn;Lmengxhu@163.com).

methodology. This term can effectively and quickly damp out the jitters nearby the sliding surface so that the system can be stable quicker than conventional SMC. For example, in [19], in order to track the motion of a piezoelectric-driven Nano-positioning system, a continuous third-order integral terminal sliding mode control (3-ITSMC) strategy based on STA is proposed. This strategy eliminates the jitters and produces a higher sliding mode precision. In this paper, the proposed 3-ITSMC performs better than traditional second-order and third-order SMC strategy in robust tracking, external disturbances restraint and other problems caused by uncertain parameters. In [20], since SMC has been widely applied to design controllers or observers in control system, Moreno et al. give a theory to construct strict Lyapunov functions, which ascertains that the proposed sliding surface is accessible and the system will become stable in finite steps. And it is proved by strict Lyapunov functions that the general system with the form of STA is stable. The proposed control strategies based on STA have greatly reduced the chartering problems caused by conventional SMC.

However, the controller methods based on STA have not been widely researched and applied. For example, few papers describe the problems of speed tracking control for DC motor systems with uncertain parameters and external disturbances based on STA. Though higher-order SMC can already effectively reduce the chattering, its structure is complicated and hard to realize or applied into industry. Hence, it's of great importance to study this kind of methodologies especially SSTSMC strategy.

Through the analysis of the above papers, the model of DC motor system with switching channels and external disturbances is constructed in this paper. The switching of channels obeys Markov jump. Then, a STO is presented to eliminate the errors of system states which are induced by switching channels and external disturbances. Based on the STO, a SSTSMC algorithm is designed to track the speed of DC motor. A nonlinear term with the form of STA is introduced in the algorithm to better reduce the jitters generated from switching channels. Finally, the proposed control method is carried out through numerical simulations and practical experiments. The results illustrate the effectiveness.

This paper mainly consists of the following parts. In Section II, the problems of speed tracking control of DC motor system are formulated. The system with multiple channels and external disturbances is considered. The switching of the channels obeys Markov jump. Section III proposes a second order super twisting controller based on STO. Section IV includes the numerical simulations and practical experiments, which are conducted to depict the availability of the proposed methodology of this paper. The last part, section V summarizes the conclusions of this paper.

II. Problem Formulation

The state-space model of DC motor system is introduced in this part, and the switching problem of multiple transmission channels that may occur in the networked control scenario is considered. Also, external disturbances are considered at the same time.

A. System Description and Modelling

The composition of the DC motor with switching channels and external disturbances is shown in Fig. 1. The system is made up of a controller and a DC motor plant. The controller calculates the suitable control value based on the measured signal, which is digital value. This value transmits through transmission channels to the DC motor after the conversion from digital to analogy. During which, there are multiple transmission channels. Each channel has different channel characteristics and transmission errors. In order to handle this problem, assume that the selection of channels is a stochastic process, in which jitters will be inevitably introduced.

Consider the two-dimensional system as follow [22]:

$$x(k+1) = Ax(k) + Bu(k) + w(k) \tag{1}$$

$$\zeta(k) = y_i(k) = C_i x(k) \tag{2}$$

where $x(k)=[x_1(k)\ \ x_2(k)]^T \in R^n$, $u(k) \in R^m$, and $y_i(k) \in R^q$ are the system states, control input, and output value severally. Meanwhile, $w(k) = \left[w_1(k)\ \ w_2(k)\right]^T \in R^w$ represents the external disturbances. A , B is the system parameter dependent matrix with appropriate dimensions. C_i is the constant matric with appropriate dimensions of channel i . The differences between $C_1, C_2, \cdots C_n$ are set to simulate the different quantifying errors and measuring noises between channels.

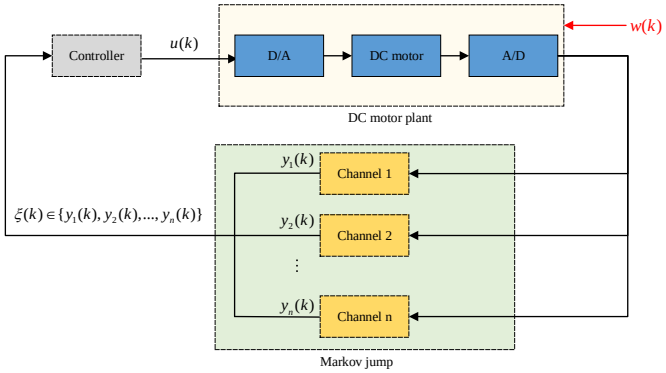

Fig. 1. DC motor system with Multi-channels and external disturbances.

According to the stochastic communication protocol (SCP) covered in [21], during the process of a single data transmission, only one channel $\xi(k) \in \{y_1(k), y_2(k), ..., y_n(k)\}$, that is, the data of one channel, can be selected to transmit data.

Assumption 1: The selection of $\xi(k)$ is a stochastic process which obeys markov jump [21].

Based on Assumption 1, under the condition of $\xi(k) = i$, the probability of $\xi(k+1) = j$ occurrence is expressed by the following relationship:

$$\mathrm{Prob}\{\xi(k+1) = j \mid \xi(k) = i\} = \pi_{ij}(k) \tag{3}$$

where $\pi_{ij}(k) \geq 0, (i, j \in \{1, 2, ..., n\})$ denotes the conditional transition probability from $\xi(k) = i$ of k time to $\xi(k+1) = j$ of $k+1$ time. Also, it satisfies

$$\sum_{j=1}^{n} \pi_{ij}(k) = 1, (i \in \{1, 2, ..., n\}) \tag{4}$$

B. External Disturbance Estimation

The term of external disturbance $w(k)$ in (1) can be estimated as follow:

$$\hat{w}(k) = w(k-1) = x(k) - Ax(k-1) - Bu(k-1) \tag{5}$$

Thus, combining (5) with the state-space equation of (1), following results can be obtained:

$$x(k+1) = Ax(k) + Bu(k) + \hat{w}(k) - \tilde{w}(k) \tag{6}$$

where $\tilde{w}(k) = \hat{w}(k) - w(k)$ is the disturbance estimation error. Hence, according to (5), $\tilde{w}(k)$ can be formulated as follow:

$$\begin{aligned} \tilde{w}(k) &= w(k-1) - w(k) \\ &= A[x(k) - x(k-1)] + B[u(k) - u(k-1)] - [x(k+1) - x(k)] \end{aligned} \tag{7}$$

Define $x(k) - x(k-1)$ as $\triangle x(k)$, $u(k) - u(k-1)$ as $\triangle u(k)$, so that (7) can be written as

$$\tilde{w}(k) = A\triangle x(k) + B\triangle u(k) - \triangle x(k+1) \tag{8}$$

Remark 1: Supposing that $x(k)$ and $u(k)$ are both bounded, it's mathematically obvious that the $\tilde{w}(k)$ is bounded as well.

III. Second-Order Super Twisting Sliding Mode Control Based on Super Twisting Observer

In this part, a STO is presented to estimate the system states and errors induced by external disturbances and channel switch. Base on this, a SSTSMC strategy is designed to better track the speed of the DC motor system.

A. Design of Observer

In the state-space model of (1)(2), only the output value $\zeta(k)$ is available. While it is essential to obtain the state values when design controller. Thus, define the errors of system states as follows:

$$e_1(k) = \hat{x}_1(k) - x_1(k) \tag{9}$$

$$e_2(k) = \hat{x}_2(k) - x_2(k) \tag{10}$$

where $\hat{x}(k) = \left[\hat{x}_1(k) \;\; \hat{x}_2(k)\right]^T$. Let $A = \begin{bmatrix} a_{11} & a_{12} \\ a_{21} & a_{22} \end{bmatrix}$, $B = \begin{bmatrix} b_1 \\ b_2 \end{bmatrix}$, equation (1) can be represented as

$$\begin{bmatrix} x_1(k+1) \\ x_2(k+1) \end{bmatrix} = \begin{bmatrix} a_{11} & a_{12} \\ a_{21} & a_{22} \end{bmatrix} \begin{bmatrix} x_1(k) \\ x_2(k) \end{bmatrix} + \begin{bmatrix} b_1 \\ b_2 \end{bmatrix} u(k) + \begin{bmatrix} w_1(k) \\ w_2(k) \end{bmatrix} \tag{11}$$

which equals as follow:

$$x_1(k+1) = a_{11}x_1(k) + a_{12}x_2(k) + b_1u(k) + w_1(k) \tag{12}$$

$$x_2(k+1) = a_{21}x_1(k) + a_{22}x_2(k) + b_2u(k) + w_2(k) \tag{13}$$

Then the STO can be designed as

$$\hat{x}_1(k+1) = a_{11}\hat{x}_1(k) + a_{12}\hat{x}_2(k) + b_1u(k) + z_1 \tag{14}$$

$$\hat{x}_2(k+1) = a_{21}\hat{x}_1(k) + a_{22}\hat{x}_2(k) + b_2u(k) + z_2 \tag{15}$$

$$\hat{y}_i(k) = C_i\hat{x}(k) \tag{16}$$

where $z_1 = k_1\left|e_1(k)\right|^{\frac{1}{2}} sign(e_1(k)) + k_2e_1(k)$ and $z_2 = k_3 sign(e_1(k)) + k_4e_1(k)$ are the correction terms.

Furthermore, according to (9) (10) and (14) (15), the error of system states can be written as

$$e_1(k+1) = a_{11}e_1(k) + a_{12}e_2(k) + z_1 - w_1(k) \tag{17}$$

$$e_2(k+1) = a_{21}e_1(k) + a_{22}e_2(k) + z_2 - w_2(k) \tag{18}$$

where $w(k)$ is bounded, k_1, k_2, k_3 and k_4 are gains that need to adjust.

Eventually, both $e_1(k+1)$ and $e_2(k+1)$ will trend to zero, under which condition the estimation states can be seen as the actual ones. That is $\hat{x}(k) = x(k)$.

According to equation (17) and (18), the error equation can be formulated as follow:

$$e(k+1) = Ge(k) + H(k)sign(e_1(k)) \tag{19}$$

where $G = \begin{bmatrix} a_{11} + k_2 & a_{12} \\ a_{21} + k_4 & a_{22} \end{bmatrix}$, $H(k) = \begin{bmatrix} k_1\left|e_1(k)\right|^{\frac{1}{2}} \\ k_3 \end{bmatrix}$.

In order to further analyze the stability and effectiveness of the mentioned method, a lemma as follow is given.

Lemma 1[23]***:*** Introduce a lambda inequality as follow:

$$M^TN + N^TM \le M^T\wp^{-1}M + N^T\wp N \tag{20}$$

Theorem 1: For given appropriate gains k_1, k_2, k_3 and k_4, if there are positive definite matrices $X = X^T > 0$, $Q = Q^T > 0$ and $\wp = \wp^T > 0$ such that the following LMI holds:

$$G^T(X + X\wp X)G - (1-\aleph)X < -Q \tag{21}$$

Then the proposed observer can be proved to be stable, and the trajectories of observation error will converge into a ball formulated as $Y_r = e : \|e\|^2 < R_d$, the center of which is at origin of the coordinates. $R_d = \dfrac{d}{1-\aleph}$ represents the radius of the ball.

where $0 < \aleph < 1$, $d = \bar{m}_2 + \dfrac{1}{4}\bar{m}_1^2\left\|Q^{-1}\right\|^2$, $\bar{m}_1 = m_1 + (k_1k_3f_{12})^2n_1$, $\bar{m}_2 = k_3^2f_{22} + (k_1k_3f_{12})^2n_1^{-1}$, $m_1 = k_1^2f_{11}$, $n_1 \in \Re^+$, $F = \begin{bmatrix} f_{11} & f_{12} \\ f_{21} & f_{22} \end{bmatrix} = \left[\wp^{-1} + X\right]$, $F, \wp, X \in \Re^{2\times2}$.

Proof: Introduce the Lyapunov function as follow:

$$V(k) = e^T(k)Xe(k) \tag{22}$$

So that

$$\begin{aligned} \triangle V(k+1) &= V(k+1) - V(k) \\ &= e^T(k+1)Xe(k+1) - e^T(k)Xe(k) \end{aligned} \tag{23}$$

According to (19), (23) can be furtherly written as

$$\begin{aligned} \triangle V(k+1) &= e^T(k)[G^TXG - X]e(k) + sign(e_1(k))H^T(k)XGe(k) \\ &\quad + H^T(k)XH(k) + e^T(k)G^TXH(k)sign(e_1(k)) \\ &= e^T(k)[G^TXG - X]e(k) + H^T(k)XH(k) \\ &\quad + 2e^T(k)G^TXH(k)sign(e_1(k)) \end{aligned} \tag{24}$$

Combining with lemma1, the term in (24) can be represented by inequation as follow:

$$\begin{aligned} &2e^T(k)G^TXH(k)sign(e_1(k)) \\ &\le e^T(k)G^TX\wp^{-1}XGe(k) + H^T(k)\wp H(k) \end{aligned} \tag{25}$$

Hence, (24) can be written as

$$\begin{aligned} \triangle V(k+1) &\le e^T(k)[G^T(X + X\wp X)G - (1-\aleph)X]e(k) \\ &\quad + H^T(k)[\wp^{-1} + X]H(k) - \wp V(k) \end{aligned} \tag{26}$$

Thus

$$\begin{aligned} H^T(k)[\wp^{-1} + X]H(k) &= H^T(k)FH(k) \\ &= \begin{bmatrix} k_1\left|e_1(k)\right|^{\frac{1}{2}} \\ k_3 \end{bmatrix}^T \begin{bmatrix} f_{11} & f_{12} \\ f_{21} & f_{22} \end{bmatrix} \begin{bmatrix} k_1\left|e_1(k)\right|^{\frac{1}{2}} \\ k_3 \end{bmatrix} \\ &= m_1\left|e_1(k)\right| + m_2\left|e_1(k)\right|^{\frac{1}{2}} + m_3 \end{aligned} \tag{27}$$

where $m_1 = k_1^2 f_{11}, m_2 = k_1 k_3 f_{12}, m_2 = k_3^2 f_{22}$.

According to lemma1, the term in equation (27) can be further represented if there exists $Q = Q^T > 0$ which satisfies the equation as follow:

$$G^T (X + X \wp X) G - (1-\aleph) X + Q = 0 \tag{28}$$

Then $\triangle V(k)$ can be written as

$$\triangle V(k+1) \le -\|e(k)\|_Q^2 + \bar{m}_1 |e_1(k)| - \aleph V(k) + \bar{m}_2 \tag{29}$$

where $\bar{m}_1 = m_1 + (k_1 k_3 f_{12})^2 n_1, \bar{m}_2 = k_3^2 f_{22} + (k_1 k_3 f_{12})^2 n_1^{-1}$.

Moreover, (29) can be further derived as follow:

$$\triangle V(k+1) \le -\|e(k)\|_Q^2 + \bar{m}_1 \|Q Q^{-1} e_1(k)\| - \aleph V(k) + \bar{m}_2 \tag{30}$$

$$\triangle V(k+1) \le -\left[\left\|Q^{\frac{1}{2}} e(k)\right\| - \frac{1}{2}\bar{m}_1 \|Q^{-1}\|\right]^T \times \left[\left\|Q^{\frac{1}{2}} e(k)\right\| - \frac{1}{2}\bar{m}_1 \|Q^{-1}\|\right] + \frac{1}{4}\bar{m}_1^2 \|Q^{-1}\|^2 - \aleph V(k) + \bar{m}_2 \tag{31}$$

That is, $$\triangle V(k+1) \le -\aleph V(k) + d \tag{32}$$

Hence, $$V(k+1) \le (1-\aleph) V(k) + d \tag{33}$$

By iterating (33), the following conclusion can be obtained:

$$V(k+1) \le (1-\aleph)^k V(0) + \sum_{j=0}^{k} (1-\aleph)^{j-1} d \tag{34}$$

Inequation (34) indicates that the observation error is convergent. Furthermore, after finite steps k, $\lim_{k \to N} V(k) \le \frac{d}{1-\aleph}$, N is a finite number. While $R_d \le \frac{d}{1-\aleph}$, which means the trajectories of observation error is converged into a ball. This finishes the proof.

B. Design of SSTSMC

The error of output defines as follow:

$$\varepsilon(k) = \zeta(k) - y_r(k) \tag{35}$$

where $\zeta(k)$ is the actual output speed of the DC motor system, while $y_r(k)$ is the reference input speed. The sliding mode function of discrete-time is designed as follow:

$$s(k) = \lambda_1 \varepsilon(k) + \lambda_2 \sum_{\tau = t_1(k)}^{t_2(k)} sig^{\partial}(\varepsilon(\tau)) + \lambda_3 \triangle \varepsilon(k) \tag{36}$$

where $\begin{cases} t_1(k) = \max\{k-10, 0\} \\ t_2(k) = \max\{k-1, 0\} \end{cases}$, $\lambda_1 > 0$, $\lambda_2 > 0$, $\lambda_3 > 0$, $0 < \partial < 1$ are the gain parameters. And $sig^{\partial}(\kappa)$, $\triangle \varepsilon(k)$ are defined by $sig^{\partial}(\kappa) \triangleq |\kappa|^{\partial} sign(\kappa)$, $\triangle \varepsilon(k) \triangleq \varepsilon(k) - \varepsilon(k-1)$.

Remark 2: The parameters $t_1(k), t_2(k)$ in equation (36) are variables, which limit the data length of the sum term in (36) and ensure that only the recent ten data will be summed (if exists), which can effectively reduce the instability caused by residual accumulation. For short, let $t_1 = t_1(k), t_2 = t_2(k)$.

Assumption 2: The error value of reference input and actual output $\varepsilon(i)$=0， $i \le 0$, the control input $u(i)$=0， $i \le 0$.

Thus, $s(k+1)$ can be formulated as follow:

$$s(k+1) = \lambda_1 \varepsilon(k+1) + \lambda_2 \sum_{\tau = t_1}^{t_2} sig^{\partial}(\varepsilon(\tau)) + \lambda_3 \triangle \varepsilon(k+1) \tag{37}$$

When sliding mode is in equilibrium, $s(k+1) = 0$, which is

$$\lambda_1 \varepsilon(k+1) + \lambda_2 \sum_{\tau = t_1}^{t_2} sig^{\partial}(\varepsilon(\tau)) + \lambda_3 \triangle \varepsilon(k+1) = 0 \tag{38}$$

Further, substitute (35), (36) into (38), it can derivate that

$$\begin{aligned} s(k+1) &= \lambda_1 \varepsilon(k+1) + \lambda_2 \sum_{\tau = t_1}^{t_2} sig^{\partial}(\varepsilon(\tau)) + \lambda_3 (\varepsilon(k+1) - \varepsilon(k)) \\ &= (\lambda_1 + \lambda_3) \varepsilon(k+1) + \lambda_2 \sum_{\tau = t_1}^{t_2} sig^{\partial}(\varepsilon(\tau)) - \lambda_3 \varepsilon(k) \\ &= (\lambda_1 + \lambda_3)(\zeta(k+1) - y_r(k+1)) + \lambda_2 \sum_{\tau = t_1}^{t_2} sig^{\partial}(\varepsilon(\tau)) - \lambda_3 \varepsilon(k) \\ &= (\lambda_1 + \lambda_3)(C_i (A\hat{x}(k) + B u_{eq}(k)) - y_r(k+1)) \\ &\quad + \lambda_2 \sum_{\tau = t_1}^{t_2} sig^{\partial}(\varepsilon(\tau)) - \lambda_3 \varepsilon(k) \\ &= 0 \end{aligned} \tag{39}$$

So, the equivalent control input equation is

$$u_{eq}(k) = B^{-1}[C_i^{-1}(\frac{-\lambda_2 \sum_{\tau = t_1}^{t_2} sig^{\partial}(\varepsilon(\tau)) + \lambda_3 \varepsilon(k)}{(\lambda_1 + \lambda_3)} + y_r(k+1)) - A\hat{x}(k)] \tag{40}$$

While the whole equivalent control law is selected as the following form:

$$u(k) = u_{eq}(k) + u_s(k) \tag{41}$$

where $u_s(k)$ is the control input with the form of STA.

Hence, $u_s(k)$ can be designed as follow:

$$u_s(k) = -\Gamma_1 |s(k)|^{\frac{1}{2}} sign(s(k)) + z(k) \tag{42}$$

$$z(k+1) = -\Gamma_2 sign(s(k)) \tag{43}$$

where $\Gamma_1 > 0$ and $\Gamma_2 > 0$ are the constant gains which need to be designed.

Remark 3: On the account of $u_s(k)$ has the form of STA, it is proved as above that the form is mathematically stable.

C. Analysis of the System Motion

Definition 1: If given inequation as follow is satisfied, then the sliding motion accessibility is proved.

$$|s(k+1)| \le |s(k)| \tag{44}$$

Theorem 2: If the abovementioned inequation is satisfied, for the discrete-time system in (1), the sliding mode function in (36), as well as the equivalent control law in (41), the trajectories of the system will finally arrive into the sliding mode bandwidth within finite steps.

Proof: Proof process can be separated into two steps: sliding motion accessibility and convergence in finite steps.

$$\begin{aligned} \varepsilon(k+1) &= \zeta(k+1) - y_r(k+1) \\ &= C_i \hat{x}(k+1) - y_r(k+1) \\ &= C_i A\hat{x}(k) + CBu(k) - y_r(k+1) \end{aligned} \tag{45}$$

According to (40) and (41), (45) can be rewritten as

$$\varepsilon(k+1)=\frac{-\lambda_2\sum_{\tau=t_1}^{t_2} sig^{\partial}(\varepsilon(\tau))+\lambda_3\varepsilon(k)}{(\lambda_1+\lambda_3)}+C_iBu_s(k) \tag{46}$$

Furthermore,

$$\begin{aligned}\triangle\varepsilon(k+1)&=\varepsilon(k+1)-\varepsilon(k)\\&=\frac{-\lambda_2\sum_{\tau=t_1}^{t_2} sig^{\partial}(\varepsilon(\tau))+\lambda_3\varepsilon(k)}{(\lambda_1+\lambda_3)}+C_iBu_s(k)\\&\quad-\frac{-\lambda_2\sum_{\tau=t_1}^{t_2} sig^{\partial}(\varepsilon(\tau))+\lambda_3\varepsilon(k-1)}{(\lambda_1+\lambda_3)}-C_iBu_s(k-1)\\&=\frac{-\lambda_2 sig^{\partial}(\varepsilon(k))+\lambda_3\triangle\varepsilon(k)}{(\lambda_1+\lambda_3)}+C_iB\triangle u_s(k)\end{aligned} \tag{47}$$

Case 1: When $s(k)\ge 0$

$$\begin{aligned}&s(k+1)-s(k)\\&=\lambda_1\varepsilon(k+1)+\lambda_2\sum_{\tau=t_1}^{t_2} sig^{\partial}(\varepsilon(\tau))+\lambda_3\triangle\varepsilon(k+1)\\&\quad-\lambda_1\varepsilon(k)-\lambda_2\sum_{\tau=t_1}^{t_2} sig^{\partial}(\varepsilon(\tau))-\lambda_3\triangle\varepsilon(k)\\&=\lambda_1\triangle\varepsilon(k+1)+\lambda_2 sig^{\partial}(\varepsilon(k))+\lambda_3(\triangle\varepsilon(k+1)-\triangle\varepsilon(k))\\&=(\lambda_1+\lambda_3)\triangle\varepsilon(k+1)+\lambda_2 sig^{\partial}(\varepsilon(k))-\lambda_3\triangle\varepsilon(k)\end{aligned} \tag{48}$$

Substitute $\triangle\varepsilon(k+1)$ into (48), it can be written as

$$s(k+1)-s(k)=(\lambda_1+\lambda_3)CB\triangle u_s(k) \tag{49}$$

$$\begin{aligned}&\triangle u_s(k)=u_s(k)-u_s(k-1)\\&=\Gamma_1|s(k)|^{\frac{1}{2}}sign(s(k))+z(k)-\Gamma_1|s(k-1)|^{\frac{1}{2}}sign(s(k-1))\\&\quad-z(k-1)\\&=\Gamma_1\left[s(k)^{\frac{1}{2}}-s(k-1)^{\frac{1}{2}}\right]+\Gamma_2 sign(s(k-1))-\Gamma_2 sign(s(k-2))\\&=\Gamma_1\left[s(k)^{\frac{1}{2}}-s(k-1)^{\frac{1}{2}}\right]\end{aligned} \tag{50}$$

Hence,

$$s(k+1)-s(k)=(\lambda_1+\lambda_3)C_iB\Gamma_1\left[s(k)^{\frac{1}{2}}-s(k-1)^{\frac{1}{2}}\right] \tag{51}$$

where $\lambda_1,\lambda_3,\Gamma_1\ge 0$, C_iB is the parameter of the plant, $(\lambda_1+\lambda_3)C_iB\Gamma_1\ge 0$.

Thus, if $s(k)-s(k-1)\le 0$, $s(k+1)-s(k)\le 0$ can be substituted.

$$\begin{aligned}s(1)-s(0)&=\lambda_1(\varepsilon(1)-\varepsilon(0))+\lambda_2 sig^{\partial}(\varepsilon(0))\\&\quad+\lambda_3(\varepsilon(1)-2\varepsilon(0)+\varepsilon(-1))\end{aligned} \tag{52}$$

According to assumption 2, $\varepsilon(0)=\varepsilon(-1)=0$, so that

$$\begin{aligned}s(1)-s(0)&=\lambda_1\varepsilon(1)+\lambda_3\varepsilon(1)\\&=(\lambda_1+\lambda_3)\cdot(\zeta(1)-y_r(1))\\&=(\lambda_1+\lambda_3)\cdot(C_i(A\hat{x}(0)+Bu(0)-y_r(1))\end{aligned} \tag{53}$$

where $\hat{x}(0)=\left[\hat{x}_1(0)\ \ \hat{x}_2(0)\right]^T=u(0)=0$, $\lambda_1,\lambda_3,y_r(1)\ge 0$, so that $s(1)-s(0)\le 0$.

Substitute $s(1)-s(0)\le 0$ into (51), so that $s(2)-s(1)\le 0$, $s(3)-s(2)\le 0,\cdots$, $s(k+1)-s(k)\le 0$ can be proved ordinally.

Case 2: When $s(k)\le 0$, it can be concluded similarly that $s(k+1)-s(k)\ge 0$.

Combining with the above two cases, it has been proved that

$$|s(k+1)|\le|s(k)| \tag{54}$$

According to definition 1, this finishes the proof of sliding motion accessibility.

Assume $s(k)\ge 0$, as proved above $s(1)-s(0)\le 0$, thus $s(1)-s(0)\le s(1)^{\frac{1}{2}}-s(0)^{\frac{1}{2}}\le 0$. If define $s(1)-s(0)=\varpi\le 0$, $(\lambda_1+\lambda_3)C_iB\Gamma_1=\delta$, so that

$$s(2)-s(1)=\delta\left[s(1)^{\frac{1}{2}}-s(0)^{\frac{1}{2}}\right]\ge\delta\varpi \tag{55}$$

After iteration it can reach that

$$s(k+1)-s(k)=\delta\left[s(k)^{\frac{1}{2}}-s(k-1)^{\frac{1}{2}}\right]\ge\delta^k\varpi \tag{56}$$

While $s(k+1)-s(k)\le 0$, so that

$$\delta^k\varpi\le s(k+1)-s(k)\le 0 \tag{57}$$

Taking step as $\tau>0$, after finite steps k, the sliding motion will come to equilibrium state, so that convergence time $T\le|\delta^k\varpi|/\tau$. While $s(k)\le 0$, it can be concluded similarly that convergence time $T\le|\delta^k\varpi|/\tau$. This finishes the proof.

IV. Simulations and Experiments Results

A. Numerical simulations

In this subsection, the numerical simulation based on DC motor system is simulated through numerical simulation as Fig.2 depicts, which is done to prove the effectiveness of the proposed methodology.

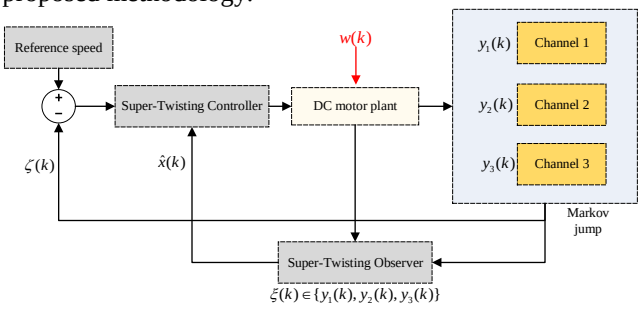

Fig. 2. DC motor system with Multi-channels and external disturbances.

The plant can be represented as (1)(2). The parameters of the plant are list as follow: $A=\begin{bmatrix}0.9647 & -0.0282\\ 0.0196 & 0.9997\end{bmatrix}$, $B=\begin{bmatrix}0.0196\\ 0.0002\end{bmatrix}$, $C_0=\begin{bmatrix}-0.2293\\ 1.4393\end{bmatrix}^T$, $C_1=\begin{bmatrix}-0.2\\ 1.4\end{bmatrix}^T$, $C_2=\begin{bmatrix}-0.25\\ 1.45\end{bmatrix}^T$. External

disturbance $w(k)=\begin{bmatrix} w_1(k) \\ w_2(k) \end{bmatrix}$, $w_1(k)=3rand(k)+\sin(k)$, $w_2(k)=rand(k)+\cos(2k)$, $rand(k)\in[0,1]$. The parameters of the STO are set as $k_1=-5, k_2=-0.6, k_3=1, k_4=0.2$. Also, the sliding mode function: $\lambda_1=900, \lambda_2=150,\ \lambda_3=100, \partial=0.3$.

The STC is set as $\Gamma_1=65, \Gamma_2=8000$. The transfer matrix of markov jump is $\pi(k)=\begin{bmatrix} 0.3 & 0.4 & 0.3 \\ 0.7 & 0.2 & 0.1 \\ 0.6 & 0.2 & 0.2 \end{bmatrix}$. Simulation time is set to be 30s, and the sampling period is 0.02s, so that there are 1500 sampling points totally. The initial conditions are as follow: $x(0)=[500\ 500]^T$, $\hat{x}(0)=[0\ 0]^T$, $u(0)=0$, $y_r(0)>0$.

The simulation results are explained as follow.

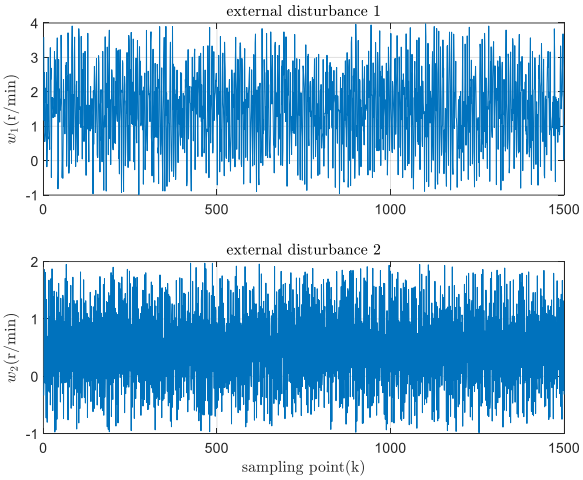

Fig.3. External disturbances of the DC motor system.

Fig.3 depicts the external disturbances added into the DC motor system, which are sinusoidal noises in general. There are 2 system states in total, external disturbance 1, 2 are injected to $x_1(k)$ and $x_2(k)$ respectively.

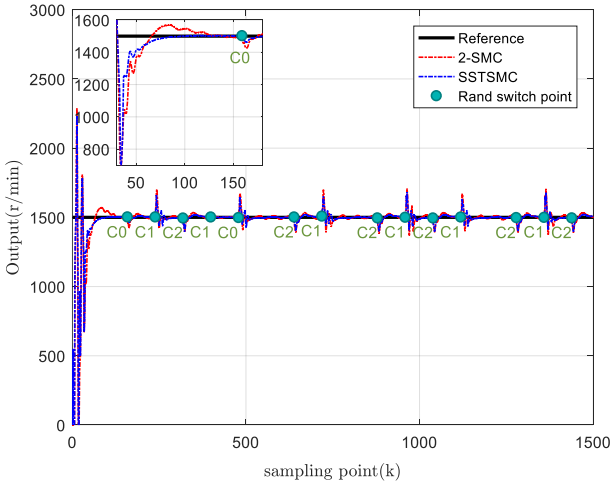

Fig.4. Output trajectories of the DC motor system at fixed speed.

Fig.4 shows the tracking output at the speed of 1500 r/min with random switch points (RSP). At about 100th sampling point (about 2s), the system starts to become stable. Meanwhile, the proposed method is better than conventional second order sliding mode control (2-SMC) algorithm in [19]. When channel changes, the proposed method performs faster and jitters smaller. Also, it has smaller static errors and jitters.

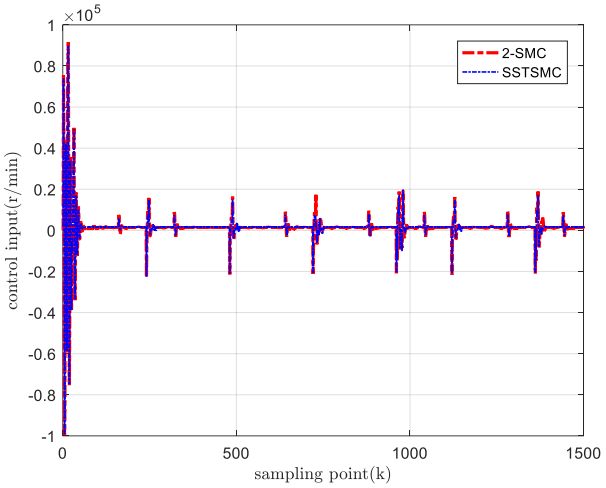

Fig.5. Trajectories of the control input at fixed speed.

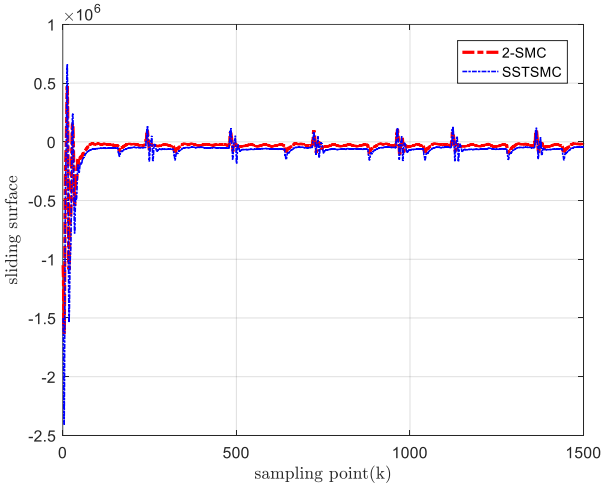

Fig.6. Sliding motion at fixed speed.

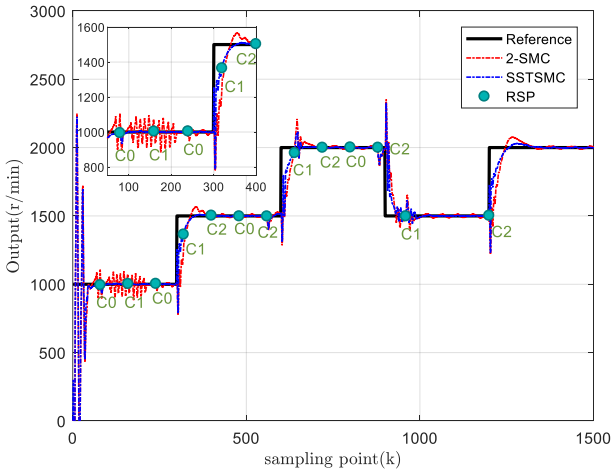

Fig.7. Output trajectories of the DC motor system at changed speed.

Fig.5 describes the trajectories of the control input. It's obvious that the proposed method consumes less energy to

reach aimed speed when transmission channel changes. Fig.6 represents the sliding motion of the two methods at fixed speed of 1500 r/min. The sliding motion will gradually come close to sliding surface, jittering in the sliding bandwidth. Also, it can be illustrated that the proposed SSTSMC jitters smaller and becomes stable quicker when channel switches.

Furthermore, to more profoundly compare these two methods, a further simulation at changed speed is carried out.

Fig.7 shows the output trajectories of the DC motor system with speed changing from 1000 r/min to 2000 r/min. At about 100^{th} sampling point (about 2s), the system of proposed method becomes stable, while the compared method keeps jittering until 200^{th} sampling point (about 4s) then it starts to be stable.

Furthermore, when the speed or transmission channel changes, the proposed method performs quicker and jitters smaller. Meanwhile, it has smaller static jitters when stabilization.

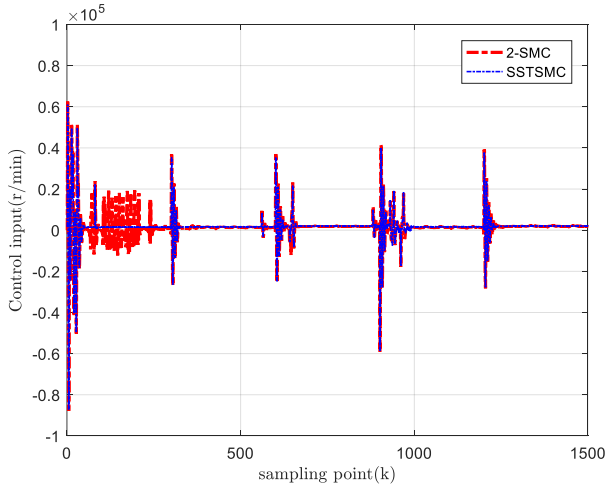

Fig.8. Trajectories of the control input at changed speed.

Fig.8 shows the trajectories of the control input at changed speed. Obviously, the proposed method wastes less energy to stabilize and has fewer static jitters.

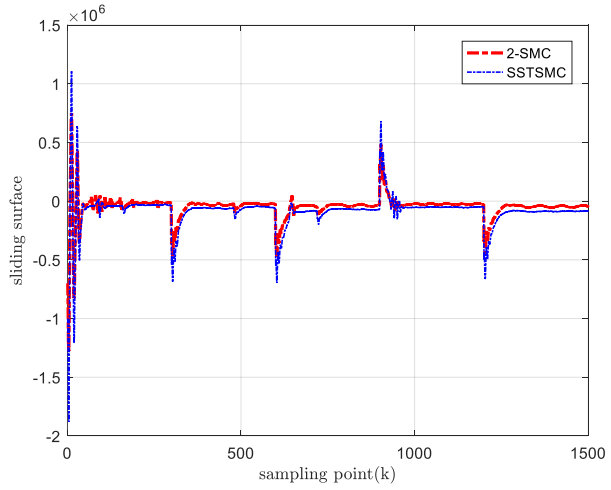

Fig.9. Sliding motion at changed speed.

Fig.9 describes the sliding motion of these two methods with speed varying from 1000 r/min to 2000 r/min. Similar to the conclusions in Fig.6, the proposed SSTSMC has smaller jitters when speed keeps unchanging. Meanwhile, when the speed or channel changes, the proposed method responses quicker.

B. Practical Experiments

In this subsection, the simulations of the DC motor system are carried out on the NetController plant. As is shown in Fig.10, the plant is made up of a DC motor, a NetController and a computer. Firstly, download the model from simulation software to the NetController through computer operation. Then the plant can start to work. The states, parameters and waves can be obtained on the computer, which are sent back from NetController through network.

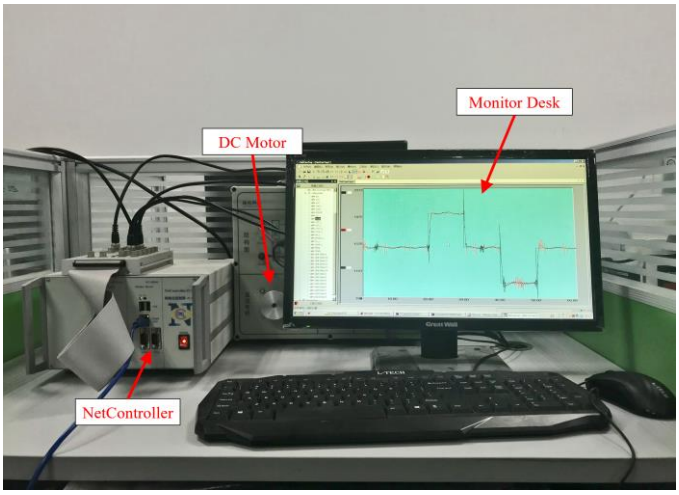

Fig.10. DC motor system with networked controller.

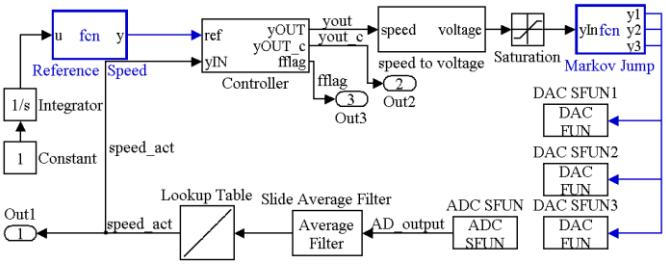

Fig.11. Simulink model of the DC motor system.

Fig.11 shows the Simulink model of the system. The changing reference speed is obtained through different time periods, the controller receives reference speed and feedback speed as input value so that it can calculate the appropriate output value. The value converts from speed value to voltage one due to the DC motor plant accepting voltage value as input. The voltage value then transmits into Markov jump function, in which determines which of the three channels the signal is output from, the selection of the channels obeys Markov jump. Thus, the chattering problems caused by channel switch can be further researched.

To carry out the experiment, the parameters of the DC motor are required firstly, which are obtained through plant identification. The parameters and variables are the same with those in subsection A. The time of experiment is set as 60s (3000 sampling points). The fixed speed tracking results are shown as Fig.12-Fig.14.

Fig.12 describes the output trajectories of the experimental plant at the speed of 2000 r/min. The differences between these two methods are tiny. However, it's still clear that the proposed methodology performs better than the compared one through partial enlarged figure.

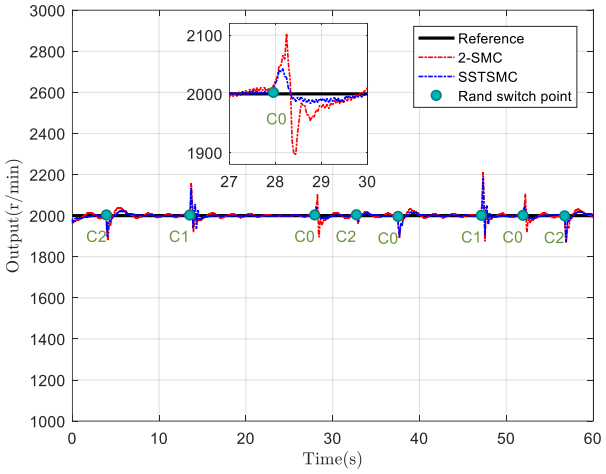

Fig.12. Output trajectories of the plant at fixed speed.

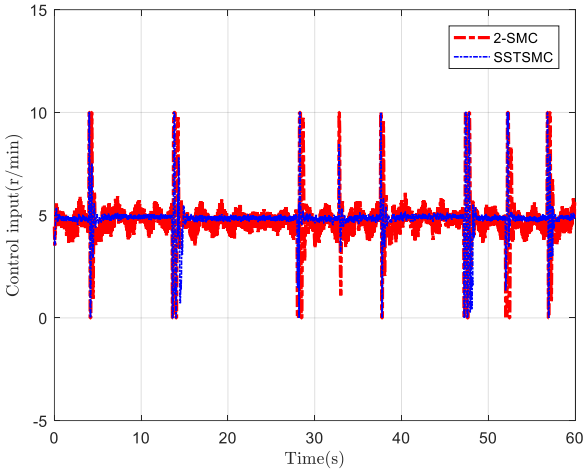

Fig.13. Trajectories of the control input of the plant at fixed speed.

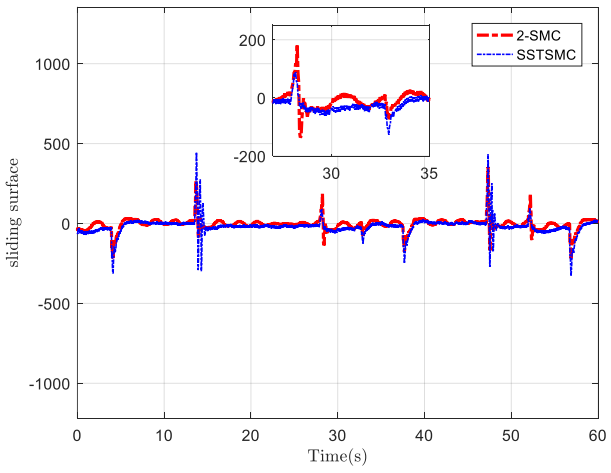

Fig.14. Sliding motion at fixed speed.

Fig.13 shows the trajectories of control input, the voltage of which is limited to 0-10V due to the input voltage range of the DC motor plant. The proposed method jitters smaller than the compared one. While channel changes, the 2-SMC method occurs larger jitters. Moreover, the static jitter of 2-SMC is more obvious. Fig.14 shows the sliding motion at fixed speed of 2000 r/min. It is clearly illustrated that SSTSMC jitters smaller when channels maintain unchangeable.

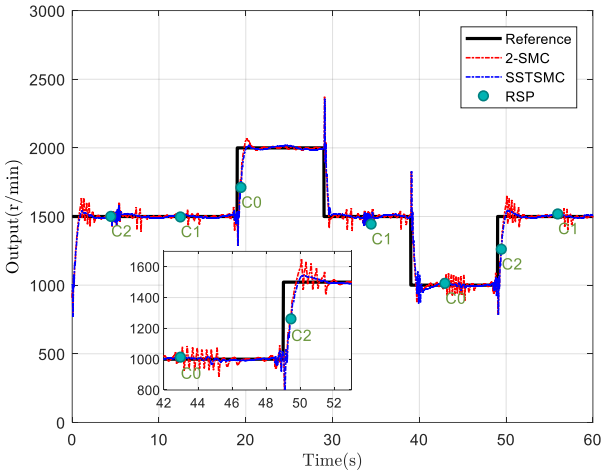

Fig. 15. Output trajectories of the plant at changed speed.

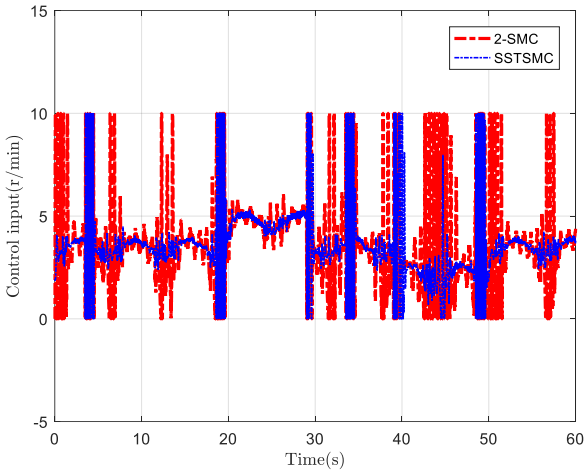

Fig. 16. Trajectories of the control input of the plant at changed speed.

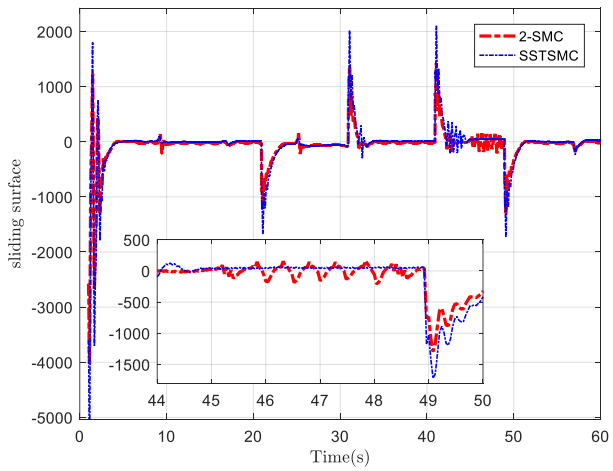

Fig. 17. Sliding motion changed speed.

Furthermore, an experiment of these two methods with speed varying from 1000 r/min to 2000 r/min is carried out. The

results of which are shown in Fig.15, Fig.16 and Fig.17. It can be seen obviously from the Fig.15 and Fig.16 as above that the compared method occurs jitters frequently even when there is no RSP. Also, when transmission channel switches or speed changes, the compared method jitters larger. The control input of 2-SMC is larger than SSTSMC. More importantly, the compared 2-SMC algorithm sometimes like 50^{th} second, appears drastically chattering while the propose SSTSMC method trends to be stable. The control input in Fig.16 can also illustrate this problem that the proposed SSTSMC strategy consumes less input energy than 2-SMC does to keep the system stable. The sliding motion in Fig.17 clarifies the problems as well.

V. Conclusion

In this paper, a DC motor system with switching channels and external disturbances is considered. As a result of which, the instability and jitters are also introduced. To solve these problems, firstly a DC motor model based on markov jump is researched. Then, a STO is presented to estimate the states. Furthermore, a SSTSMC based on STA is presented. The reachability of sliding surface and convergence in finite steps as well as the stability of the controller are mathematically testified. In the end, the proposed control method is carried out on numerical simulations and practical NetController plant. Both results SSTSMC method in this paper is more reliable and better than conventional 2-SMC strategy.

References

[1] A. Lee, C. Fan and G. Chen, "Current Integral Method for Fine Commutation Tuning of Sensorless Brushless DC Motor," *IEEE Transactions on Power Electronics*, vol. 32, no. 12, pp. 9249-9266, Dec. 2017.

[2] L. Zhang, X. Yin, Z. Ning and D. Ye, "Robust filtering for a class of networked nonlinear systems with switching communication channels," IEEE *Transactions on Cybernetics*, vol. 47, no. 3, pp. 671-682, Mar. 2017.

[3] Z. Wu, P. Shi, Z. Shu, H. Su and R. Lu, "Passivity-based asynchronous control for Markov jump systems," *IEEE Transactions on Automatic Control*, vol. 62, no. 4, pp. 2020-2025, Apr. 2017.

[4] X. Yin, L. Zhang, Y. Zhu, C. Wang and Z. Li, "Robust control of networked systems with variable communication capabilities and application to a semi-active suspension system," *IEEE/ASME Transactions on Mechatronics*, vol. 21, no. 4, pp. 2097-2107, Aug. 2016.

[5] J. Zhu, X. Yu, T. Zhang, et al. "Sliding mode control of MIMO Markovian jump systems." *Automatica*, vol. 68, pp. 286-293, Jun. 2016.

[6] H. Youness, M. Moness and M. Khaled, "MPSoCs and multicore microcontrollers for embedded PID control: a detailed study," *IEEE Transactions on Industrial Informatics*, vol. 10, no. 4, pp. 2122-2134, Nov. 2014.

[7] G. Rigatos, P. Siano, A. Melkikh and N. Zervos, "A nonlinear H-infinity control approach to stabilization of distributed synchronous generators," *IEEE Systems Journal*, vol. 12, no. 3, pp. 2654-2663, Sept. 2018.

[8] Z. Du, D. Yue and S. Hu, "H-infinity stabilization for singular networked cascade control systems with state delay and disturbance," *IEEE Transactions on Industrial Informatics*, vol. 10, no. 2, pp. 882-894, May 2014.

[9] H. Sun, R. Yu, Y. Chen and H. Zhao, "Optimal design of robust control for fuzzy mechanical systems: performance-based leakage and confidence-index measure," *IEEE Transactions on Fuzzy Systems*, vol. 27, no. 7, pp. 1441-1455, Jul. 2019.

[10] H. Yan, Y. Xu, F. Cai, H. Zhang, W. Zhao and C. Gerada, "PWM-VSI Fault Diagnosis for a PMSM Drive Based on the Fuzzy Logic Approach," *IEEE Transactions on Power Electronics*, vol. 34, no. 1, pp. 759-768, Jan. 2019.

[11] G. P. Incremona, A. Ferrara and L. Magni, "Asynchronous networked MPC with ISM for uncertain nonlinear systems," *IEEE Transactions on Automatic Control*, vol. 62, no. 9, pp. 4305-4317, Sept. 2017.

[12] M. Zanon, L. Grüne and M. Diehl, "Periodic Optimal Control, Dissipativity and MPC," *IEEE Transactions on Automatic Control*, vol. 62, no. 6, pp. 2943-2949, Jun. 2017.

[13] R. Han, L. Meng, J. M. Guerrero and J. C. Vasquez, "Distributed Nonlinear Control with Event-Triggered Communication to Achieve Current-Sharing and Voltage Regulation in DC Microgrids," *IEEE Transactions on Power Electronics*, vol. 33, no. 7, pp. 6416-6433, July 2018.

[14] B. Demirel, A. S. Leong, V. Gupta and D. E. Quevedo, "Tradeoffs in Stochastic Event-Triggered Control," *IEEE Transactions on Automatic Control*, vol. 64, no. 6, pp. 2567-2574, Jun. 2019.

[15] S. Zou, A. Mallik, J. Lu and A. Khaligh, "Sliding Mode Control Scheme for a CLLC Resonant Converter," *IEEE Transactions on Power Electronics*, vol. 34, no. 12, pp. 12274-12284, Dec. 2019.

[16] Q. Xu, "Piezoelectric nanopositioning control using second-order discrete-time terminal sliding-mode strategy," *IEEE Transactions on Industrial Electronics*, vol. 62, no. 12, pp. 7738-7748, Dec. 2015.

[17] A. Ferrara and G. P. Incremona, "Design of an integral suboptimal second-order sliding mode controller for the robust motion control of robot manipulators," *IEEE Transactions on Control Systems Technology*, vol. 23, no. 6, pp. 2316-2325, Nov. 2015.

[18] A. Merabet, K. T. Ahmed, H. Ibrahim and R. Beguenane, "Implementation of sliding mode control system for generator and grid sides control of wind energy conversion system," *IEEE Transactions on Sustainable Energy*, vol. 7, no. 3, pp. 1327-1335, July 2016.

[19] Q. Xu, "Continuous integral terminal third-order sliding mode motion control for piezoelectric nanopositioning System," *IEEE/ASME Transactions on Mechatronics*, vol. 22, no. 4, pp. 1828-1838, Aug, 2017.

[20] J. A. Moreno and M. Osorio, "Strict lyapunov functions for the super-twisting algorithm," *IEEE Transactions on Automatic Control*, vol. 57, no. 4, pp. 1035-1040, Apr, 2012.

[21] L. Zou, Z. Wang, H. Gao, "Observer-based H∞ control of networked systems with stochastic communication protocol: The finite-horizon case," *Automatica*, vol. 63, pp. 366-373, Jan. 2016.

[22] M. Li and Y. Chen, "Robust adaptive sliding mode control for switched networked control systems with disturbance and faults," *IEEE Transactions on Industrial Informatics*, vol. 15, no. 1, pp. 193-204, Jan. 2019.

[23] L. Qiu, Y. Shi, F. Yao, G. Xu, and B. Xu, "Network-based robust H_2/H_∞ control for linear systems with two-channel random packet dropouts and time delays," *IEEE Transactions on Cybernetics*, vol. 45, no. 8, pp. 1450-1462, Aug. 2015.